Available online at www.sciencedirect.com
ScienceDirect
Journal of Solid State Chemistry 180 (2007) 1770–1774
JOURNAL OF SOLID STATE CHEMISTRY
www.elsevier.com/locate/jssc

Synthesis, structure and magnetic properties of new vanadate $PbCo_2V_2O_8$

Zhangzhen He[a,*], Yutaka Ueda[a], Mitsuru Itoh[b]

[a]*Institute for Solid State Physics, University of Tokyo, Kashiwa 277-8581, Japan*
[b]*Materials and Structures Laboratory, Tokyo Institute of Technology, 4259 Nagatsuta, Midori, Yokohama 226-8503, Japan*

Received 22 January 2007; received in revised form 26 March 2007; accepted 29 March 2007
Available online 10 April 2007

Abstract

A new vanadate $PbCo_2V_2O_8$ was obtained through the study of PbO–CoO–V_2O_5 ternary system. The crystal structure was determined by Rietveld method, indicating that $PbCo_2V_2O_8$ has a tetragonal structure of space group $I41cd$ with a spiral chain along the c-axis. Magnetic properties of the titled compound were investigated by means of susceptibility, magnetization, and heat capacity measurements. The results show that $PbCo_2V_2O_8$ is a quasi-one-dimensional canted antiferromagnet with Neel temperature of ~4 K, being consistent with its crystal structure.

Keywords: $PbCo_2V_2O_8$; Vanadates; Crystal structure; Canted antiferromagnet

1. Introduction

Compounds with a general formula of $AM_2V_2O_8$ (A = Ba, Sr, Pb; M = Cu, Ni, Co, Mn) have now attracted much interest in solid state chemistry and physics, due to the discovery of their various interesting magnetic phenomena [1–13]. For example, $BaCu_2V_2O_8$ is a quasi-one-dimensional (1D) alternating spin chain system with a large spin gap of ~230 K [1,2], while $PbNi_2V_2O_8$ is a typical 1D Haldane spin-gap system [4,5] and $BaNi_2V_2O_8$ is a prototype of two-dimensional XY system [7,8]. $BaCo_2V_2O_8$ and $SrCo_2V_2O_8$ are 1D Ising spin systems with large magnetic anisotropy [9–12], while $BaMn_2V_2O_8$ is a 1D antiferromagnet with weak ferromagnetism [13].

In this work, a new vanadate $PbCo_2V_2O_8$ which also belongs to the family of $AM_2V_2O_8$, was found through the study of PbO–CoO–V_2O_5 ternary system. The crystal structure of $PbCo_2V_2O_8$ was determined by the Rietveld method from X-ray powder diffraction data at room temperature. We found that $PbCo_2V_2O_8$ displays a spiral chain structure viewed along the c-axis. From the magnetic properties of $PbCo_2V_2O_8$ investigated by means of magnetic susceptibility, magnetization and heat capacity measurements, it is revealed that $PbCo_2V_2O_8$ is a quasi-one-dimensional canted antiferromagnet with Neel temperature of ~4 K.

2. Experimental section

A polycrystalline sample of $PbCo_2V_2O_8$ was synthesized by a standard solid-state reaction method using a mixture of high purity reagents of PbO (4 N), $CoC_2O_4 \cdot 2H_2O$ (3 N), and V_2O_5 (4 N) as the starting materials in the molar ratio of 1:2:1. The mixture was ground carefully, homogenized thoroughly with ethanol (99%) in an agate mortar, and then packed into an alumina crucible and calcined at 1173 K in air for 80 h with several intermediate grindings. Finally, the product was pressed into pellets and sintered at 1203 K for 30 h, and then cooled to room temperature at a rate of 100 K/h. Powder X-ray diffraction (XRD) data were collected at room temperature in the angular range of $2\theta = 10$–120° with a scan step width of 0.02° and a fixed counting time of 4 s using an MXP21AHF (Mac Science) powder diffractometer with graphite monochromatized CuKα radiation. Composition analysis was performed using an electron probe microanalysis (EPMA) system

*Corresponding author. Fax: +81 4 7136 3436.
E-mail address: he@issp.u-tokyo.ac.jp (Z. He).

0022-4596/$ - see front matter © 2007 Elsevier Inc. All rights reserved.
doi:10.1016/j.jssc.2007.03.026

(JEOL JSM-5600 Oxford Link ISIS). No other metal elements except for Pb, Co, and V were confirmed and the molar ratio of Pb:Co:V:O was calculated to be 1:2:2:8, which agreed with the formula of $PbCo_2V_2O_8$. The structural parameters were refined by the Rietveld method using the RIETAN-2000 program [14]. The magnetic susceptibility and magnetization were measured using a superconducting quantum interference device (MPMS5S, Quantum Design) magnetometer and the heat capacity was measured by a relaxation method using a commercial physical property measurement system (PPMS, Quantum Design).

3. Results and discussion

Indexing Bragg reflections in the XRD data indicated that $PbCo_2V_2O_8$ crystallizes in the tetragonal system. The crystal structure was refined by the Rietveld method. We found the reports about two compounds $BaCo_2V_2O_8$ (*S. G. I*41/*acd*) [15] and $SrCo_2V_2O_8$ (*S. G. I*41*cd*) [16] in the family of $AM_2V_2O_8$ with $M = Co$. Since the XRD pattern of $PbCo_2V_2O_8$ was very similar to that of $SrCo_2V_2O_8$, the structural parameters of $SrCo_2V_2O_8$ were used as initial model for structure refinement of $PbCo_2V_2O_8$. A full-matrix refinement with 39 refined parameters was performed, yielding final reliability factors $R_{wp} = 3.11\%$, $Rp = 2.50\%$, $R_F = 1.83\%$, and $S = 2.64$. Fig. 1 shows the observed and calculated XRD patterns for $PbCo_2V_2O_8$. The final structure parameters are given in Table 1, and selected bond lengths and angles are listed in Table 2.

The structural framework of $PbCo_2V_2O_8$ is very similar to that of $SrCo_2V_2O_8$. Fig. 2(a) shows the projection of the structure of $PbCo_2V_2O_8$ onto the *a*–*b* plane. Four basic structural clusters ($Co_4V_4O_{16}$) are seen in a unit cell, which

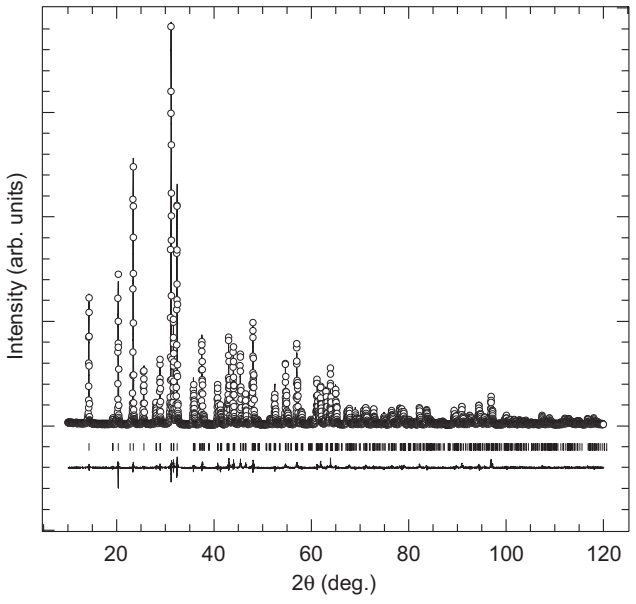

Fig. 1. Observed (open circles) and calculated (solid line) XRD pattern for $PbCo_2V_2O_8$ at room temperature. The difference is shown at the bottom and Bragg reflections are indicated by vertical marks.

Table 1
Structure parameters obtained from the Rietveld refinement of $PbCo_2V_2O_8$[a]

Atom	Wyckoff position	*x*	*y*	*z*	B_{iso} (Å)
Pb	8a[b]	0	0	0	1.58(4)
Co	16b	0.3269(3)	0.3365(2)	0.1746(1)	0.70(8)
V	16b	0.2594(1)	0.0783(8)	0.0479(1)	0.53(6)
O1	16b	0.1596(2)	0.5046(1)	−0.0494(5)	1.26(3)
O2	16b	0.3418(1)	0.6737(9)	0.4456(5)	0.32(1)
O3	16b	0.1563(5)	0.6780(9)	0.6829(5)	1.38(5)
O4	16b	0.3097(5)	0.5088(8)	0.1581(2)	1.50(6)

[a]Space group: *I*41*cd* (No. 110); $a = 12.3482(5)$ Å, $c = 8.4378(3)$ Å, $Z = 8$, $V = 1286.593(1)$ Å^3; $R_{wp} = 3.11\%$, $Rp = 2.50\%$, $R_F = 1.83\%$, and $S = 2.64$. Occupancies for all sites were assumed to be 1.0.
[b]Pb site was fixed at the origin.

Table 2
Selected interatomic distances (Å) and bond angles (°) for $PbCo_2V_2O_8$

Atoms	Distance	Atoms	Angle
Pb–O1	2.59(8) × 2	O2–Co–O1	92.86(7)
Pb–O4	2.70(4) × 2	O2–Co–O3	83.05(8)
Pb–O2	2.93(8) × 2	O2–Co–O3	87.58(1)
Pb–O3	2.98(1) × 2	O2–Co–O2	90.96(1)
Pb–O1	3.20(5) × 2	O2–Co–O4	170.31(9)
Pb–O4	3.72(2) × 2		
Co–O1	2.13(5)	O2–V–O3	111.01(1)
Co–O2	1.93(9)	O2–V–O1	112.77(4)
Co–O2	2.21(2)	O2–V–O4	98.21(9)
Co–O3	2.18(6) × 2		
Co–O4	2.15(2)	Co–O2–Co	91.13(6)
V–O1	1.58(3)	Co–O3–Co	85.56(7)
V–O2	1.79(1)		
V–O3	1.69(6)		
V–O4	1.52(7)		

contains four edge-shared CoO_6 octahedra and isolated VO_4 tetrahedra. The three-dimensional framework is built up of the basic structural clusters bridged by VO_4 tetrahedra. This framework forms large cavities, and Pb^{2+} occupies the middle of the cavities. Fig. 2(b) shows the structural cluster viewed along the *a*-axis. It is found that the structural clusters form spiral chains running along the *c*-axis, and the spiral chains are separated by VO_4 (V^{5+}) tetrahedra and Pb^{2+} ions, resulting in a quasi-one-dimensional structural arrangement. Fig. 2(c) shows a structural arrangement of isolated Co^{2+} ions onto the *a*–*b* plane. Four spiral chains are clearly seen and the nearest-neighbor chains screw adversely each other with right or left manner. Fig. 3 shows the environment around Co^{2+} and V^{5+} ions in $PbCo_2V_2O_8$.

Fig. 4 shows the temperature dependences of the magnetic susceptibility for polycrystalline $PbCo_2V_2O_8$. The susceptibility increases with decreasing temperature, while a broad maximum is observed around 30 K, showing a characteristic feature of short-range ordering in 1D magnetism. A rapid increase in susceptibility is seen around

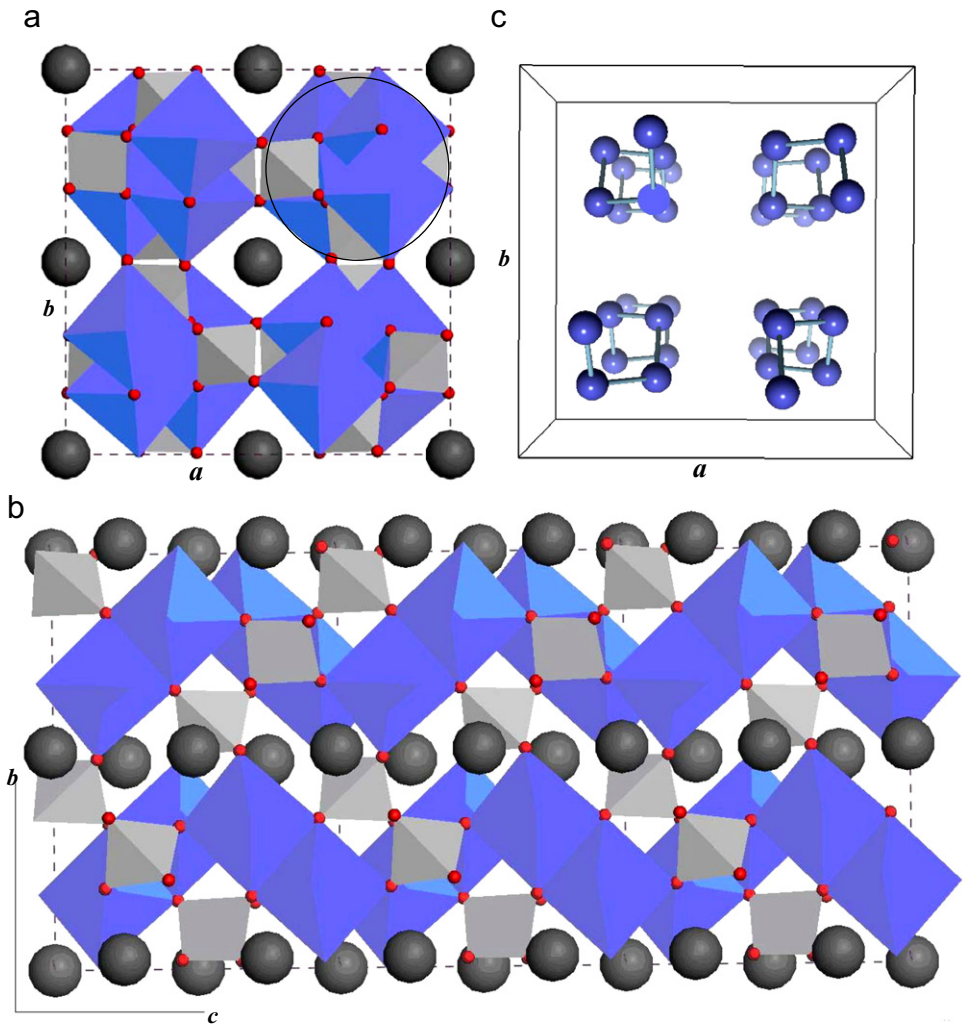

Fig. 2. (a) The projection of the structure of $PbCo_2V_2O_8$ onto the *a–b* plane. Octahedra, tetrahedra, large ball and small ball represent CoO_6, VO_4, Pb, and O, respectively. The circle shows a basic structural cluster of ($Co_4V_4O_{16}$) in a unit cell. (b) The projection of the structure of $PbCo_2V_2O_8$ onto the *b–c* plane. (c) A structural arrangement of isolated Co^{2+} ions onto the *a–b* plane.

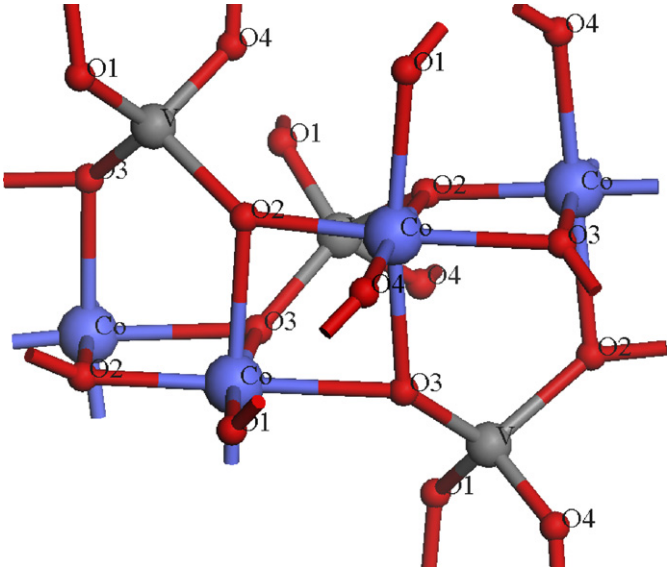

Fig. 3. The environment around Co^{2+} and V^{5+} ions in $PbCo_2V_2O_8$.

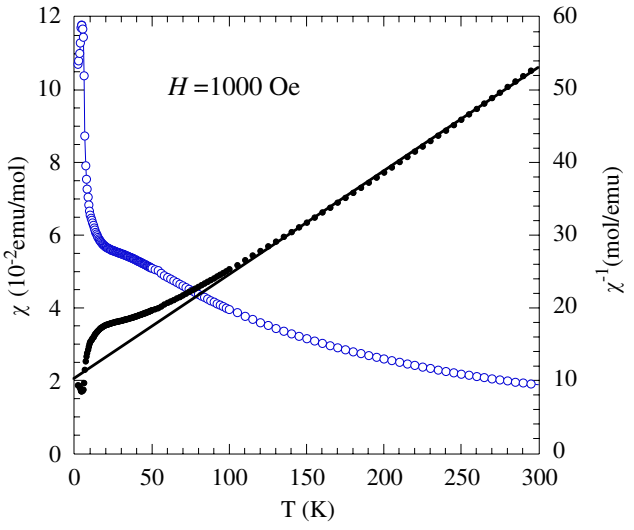

Fig. 4. Temperature dependences of the magnetic susceptibility for polycrystalline $PbCo_2V_2O_8$.

7 K, indicating the development of ferromagnetic correlations, while a sharp peak is seen at ~4 K. The ferromagnetic moment is roughly estimated to be ~0.01 μ_B/Co^{2+} in a field of 1000 Oe, which corresponds to ~0.34% of the full moments of Co^{2+} ions ($S = 3/2$). This value is too small for a ferromagnetic state, suggesting that the system falls into a canted antiferromagnet below ~4 K. The Curie constant $C = 6.95(6)$ emu K/mol and Weiss temperature $\theta = -70.7(1)$ K were obtained from the Curie–Weiss fitting of the reciprocal susceptibility in the region of 100–300 K. The effective magnetic moment of Co^{2+} ions in the system is calculated to be 5.27(5) μ_B, which is larger than the value 3.87(3) μ_B obtained by Co^{2+} ($S = 3/2$) ions, indicating a large orbital moment contribution of Co^{2+} in oxygen octahedral environment. Also, the negative Weiss temperature indicates that the interactions between magnetic Co^{2+} ions are antiferromagnetic in nature.

Fig. 5 shows the magnetization as a function of applied field (M–H) at 2 K. A magnetization rapidly increases in the low field region, showing weak ferromagnetism in the system. Further, a linear behavior of magnetization is seen at $H > 3000$ Oe, showing a characteristic feature of canted antiferromagnet, which are in good agreement with susceptibility data. The weak ferromagnetic moment (M_{WF}) of ~0.09 μ_B can be obtained by subtracting the linear component ($M_{WF} = M - \chi H$) in the magnetization (see the inset of Fig. 5) and we can also estimate the canted angle θ of 0.17(1)° by assuming the full moment (M_F) of 3 μ_B for Co^{2+} ions, based on the equation $M_{WF} = M_F \sin\theta$. Further evidence for canted AF transition at ~4 K is obtained from heat capacity data. Fig. 6 shows the results of heat capacity measurements in $H = 0$. There is a slight jump at ~7 K, followed by a clear sign of l-like feature at around 4 K, which agrees with the susceptibility data. This indicates that a long-range magnetic

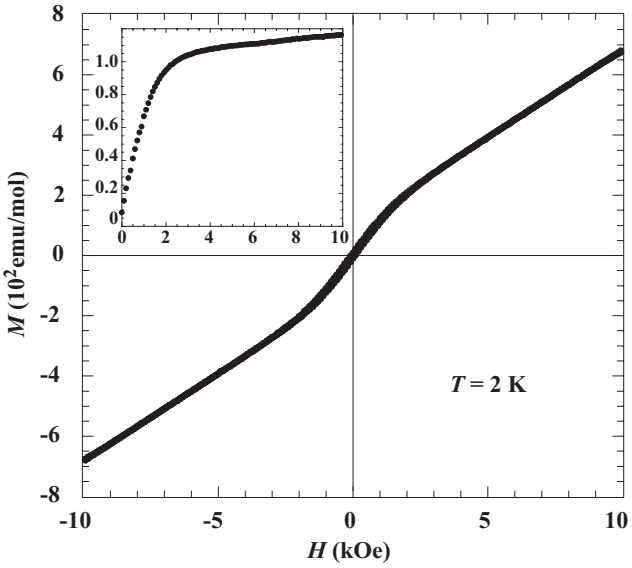

Fig. 5. Magnetization as a function of applied field H at 2 K. The inset shows weak ferromagnetic moment through subtracting the linear component in the magnetization.

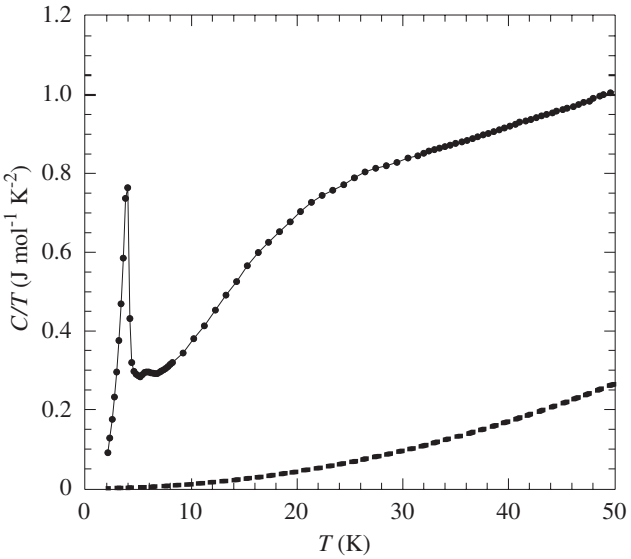

Fig. 6. Heat capacity measured in zero magnetic field. The dashed line represents the lattice contribution to heat capacity.

ordering starts at ~7 K and completes in a canted antiferromagnetic transition at ~4 K. A linear temperature dependence of C/T above 30 K shows characteristic of a uniform 1D AF chain system. The data above 30 K can be well fitted to $C_p = \gamma T + \beta T^3$ with $\gamma = 0.7463(8)$ J mol^{-1} K^{-1} and $\beta = 1.062(5) \times 10^{-4}$ J mol^{-1} K^{-4}. Since $PbCo_2V_2O_8$ is an insulator, it is reasonable to arrange the γT term to the magnetic contribution (C_m) and the βT^3 term to the lattice contribution (C_l). Therefore, the magnetic contribution below 30 K was calculated as $C_m = C_p - C_l$ and the magnetic entropy change for this λ-like anomaly around 4 K was roughly estimated to be $\Delta S = \sim 1.4$ J/mol K, which corresponds to 12.4% of $R\ln(2S+1)$ expected for spin-3/2 systems. This indicates that most of the entropy of the system has been lost through the short-range magnetic correlation as seen at ~30 K, also agreeing with the characteristic feature of 1D magnetism.

Our experimental results of the susceptibility, magnetization and heat capacity measurements clearly show that $PbCo_2V_2O_8$ is a quasi-one-dimensional canted antiferromagnet. As reported previously, weak ferromagnetism was observed in $SrCo_2V_2O_8$ with space group $I41cd$ [10], while no weak ferromagnetism was seen in $BaCo_2V_2O_8$ with space group $I41/acd$ [12]. Such weak ferromagnetism may arise from the Dzyaloshinskii–Moriya (DM) interactions [17,18], due to the noncentrosymmetric crystal structure. Therefore, weak ferromagnetism in $PbCo_2V_2O_8$ indicates that the system has a noncentrosymmetric crystal structure, agreeing with the determined structure. In addition, it is found that $PbNi_2V_2O_8$ crystallizes in the tetragonal system, which is similar to $SrNi_2V_2O_8$ with space group $I41cd$ [19] and different from $BaNi_2V_2O_8$ with space group R-3 [20]. Our results also indicate that the structures of $PbM_2V_2O_8$ are close to those of $SrM_2V_2O_8$ in the family of $AM_2V_2O_8$ mentioned above, although the radii of Pb^{2+} are between those of Ba^{2+} and Sr^{2+} [21].

4. Conclusions

A new vanadate $PbCo_2V_2O_8$ has been obtained through the study of PbO–CoO–V_2O_5 ternary system. $PbCo_2V_2O_8$ was found to crystallize in tetragonal system with space group $I41cd$, which displays an unusual spiral chain structure along the c-axis. Susceptibility, magnetization and heat capacity measurements show that $PbCo_2V_2O_8$ is a quasi-one-dimensional spin-3/2 canted antiferromagnet. The weak ferromagnetism is observed in $PbCo_2V_2O_8$, which is consistent with its noncentrosymmetric crystal structure.

Acknowledgments

The authors thank Ms. Y. Kiuchi for her assistance with EPMA measurement. One of the authors (Z.H.) acknowledges the Japan Society for the Promotion of Science (JSPS) for awarding the Foreigner Postdoctoral Fellowship (P06047).

References

[1] Z. He, T. Kyômen, M. Itoh, Phys. Rev. B 69 (2004) 220407.
[2] K. Ghoshray, B. Pahari, B. Bandyopadhyay, R. Sarkar, A. Ghoshray, Phys. Rev. B 71 (2005) 214401.
[3] C.S. Lue, B.X. Xie, Phys. Rev. B 72 (2005) 052409.
[4] Y. Uchiyama, Y. Sasago, I. Tsukada, K. Uchinokura, A. Zheludev, T. Hayashi, N. Miura, P. Böni, Phys. Rev. Lett. 83 (1999) 632.
[5] A. Zheludev, T. Masuda, I. Tsukada, K. Uchiyama, K. Uchinokura, P. Boni, S.H. Lee, Phys. Rev. B 62 (2000) 8921.
[6] B. Pahari, K. Ghoshray, R. Sarkar, B. Bandyopadhyay, A. Ghoshray, Phys. Rev. B 73 (2006) 012407.
[7] N. Rogado, Q. Huang, J.W. Lynn, A.P. Ramirez, D. Huse, R.J. Cava, Phys. Rev. B 65 (2002) 144443.
[8] M. Heinrich, H.A. Krug von Nidda, A. Loidl, N. Rogado, R.J. Cava, Phys. Rev. Lett. 91 (2003) 137601.
[9] Z. He, D. Fu, T. Kyômen, T. Taniyama, M. Itoh, Chem. Mater. 17 (2005) 2924.
[10] Z. He, T. Taniyama, T. Kyômen, M. Itoh, Phys. Rev. B 72 (2005) 172403.
[11] Z. He, T. Taniyama, M. Itoh, Appl. Phys. Lett. 88 (2006) 132504.
[12] Z. He, T. Taniyama, M. Itoh, Phys. Rev. B 73 (2006) 212406.
[13] Z. He, Y. Ueda, M. Itoh, Solid State Commun. 141 (2007) 22.
[14] F. Izumi, T. Iketa, Mater. Sci. Forum 321–324 (2000) 198.
[15] R. Wichmann, Hk. Müller-Buschbaum, Z. Anorg. Allg. Chem. 532 (1986) 153.
[16] D. Osterloh, Hk. Müller-Buschbaum, Z. Naturforsch. B 49 (1994) 923.
[17] I. Dzyaloshinskii, Sov. Phys. JETP 5 (1957) 1259.
[18] T. Moriya, Phys. Rev. 120 (1960) 91.
[19] R. Wichmann, Hk. Müller-Buschbaum, Rev. Chem. Miner. 23 (1986) 1.
[20] R. Wichmann, Hk. Müller-Buschbaum, Rev. Chem. Miner. 21 (1984) 824.
[21] R.D. Shannon, Acta Crystallogr. A 32 (1976) 751.